

Abstract

The uncertainties in the cloud physical properties derived from satellite observations make it difficult to interpret model evaluation studies. In this paper, the uncertainties in the cloud water path (CWP) retrievals derived with the cloud physical properties retrieval algorithm (CPP) of the climate monitoring satellite application facility (CM-SAF) are investigated. To this end, a numerical simulator of MSG-SEVIRI observations was developed that calculates the reflectances at 0.64 and 1.63 μm for a wide range of cloud parameters, satellite viewing geometries and surface albedos. These reflectances are used as input to CPP, and the retrieved values of CWP are compared to the original input of the simulator.

It is shown that the CWP retrievals are very sensitive to the assumptions made in the CPP code. The CWP retrieval errors are generally small for unbroken single-phase clouds with COT >10 , with retrieval errors of $\sim 3\%$ for liquid water clouds to $\sim 10\%$ for ice clouds. When both liquid water and ice clouds are present in a pixel, the CWP retrieval errors increase dramatically; depending on the cloud, this can lead to uncertainties of 40–80%. CWP retrievals also become more uncertain when the cloud does not cover the entire pixel, leading to errors of $\sim 50\%$ for cloud fractions of 0.75 and even larger errors for smaller cloud fractions. Thus, the satellite retrieval of cloud physical properties of broken clouds and multi-phase clouds is complicated by inherent difficulties, and the proper interpretation of such retrievals requires extra care.

1 Introduction

Clouds play a significant role in the climate system, since they influence the atmospheric energy balance by scattering and absorbing solar and terrestrial radiation, and by playing an key role in the atmospheric water cycle. Thus, it is important for climate models to treat clouds as accurately as possible. Comparison of model cloud physical properties with satellite observations is a valuable tool in providing accurate cloud statistics (Roebeling et al., 2006).

ACPD

12, 4311–4340, 2012

Quantifying retrieval uncertainties in CPP

B. J. Jonkheid et al.

Title Page

Abstract

Introduction

Conclusions

References

Tables

Figures

◀

▶

◀

▶

Back

Close

Full Screen / Esc

Printer-friendly Version

Interactive Discussion



Quantifying retrieval uncertainties in CPP

B. J. Jonkheid et al.

[Title Page](#)[Abstract](#)[Introduction](#)[Conclusions](#)[References](#)[Tables](#)[Figures](#)[◀](#)[▶](#)[◀](#)[▶](#)[Back](#)[Close](#)[Full Screen / Esc](#)[Printer-friendly Version](#)[Interactive Discussion](#)

Comparing model output to satellite observations can be done in several different ways, illustrated in Fig. 1. In stage I, the model cloud field is compared directly to the cloud parameters (e.g. cloud optical thickness (COT), particle effective radius (r_{eff}), cloud water path (CWP)) retrieved from the satellite observations; any discrepancies between model and retrieved properties can be easily assigned to errors in these parameters. In stage II, a synthetic satellite image is simulated from the model cloud field to compare this to the observations; while straightforward, it is not clear in this stage how to interpret differences between model and observations in terms of physical parameters. In stage III, a retrieval algorithm is used to derive the cloud physical properties from the synthetic satellite images, and these are compared to the model input; stage III is identical to stage I, except that in this stage, the satellite measured reflectances are replaced by synthetic ones. Thus, stage III is entirely decoupled from actual observations, and is useful to diagnose the model-simulator-retrieval algorithm chain. In stage IV, the cloud parameters retrieved from the satellite observations are compared with those retrieved from the synthesised observations.

The classical methodology in model evaluation is to compare model fields directly with retrieved satellite products (i.e. stage I in Fig. 1). Examples using this methodology are Molders et al. (1995), who evaluated cloud cover parametrization schemes with NOAA9 AVHRR data; Tselioudis and Jakob (2002) evaluated seasonal cloud property distributions of mid-latitude clouds in weather and climate models (ECMWF and GISS, respectively) with ISCCP observations; Roebeling and van Meijgaard (2009) evaluated diurnal variations in cloud physical properties by comparing statistics in model and satellite retrievals; and recently Greuell et al. (2011) evaluated a climate model using earth radiation budget observations from the GERB instrument and cloud physical properties from SEVIRI. The main disadvantage of such classical model evaluations is that model-to-satellite differences are partly due to model errors, partly due to inadequate satellite retrieval assumptions and finally due to intrinsic differences in the definitions of model and satellite products. Because of this entanglement of uncertainties in both the satellite retrievals and the model formulation of cloud parameters, it is

difficult to assess model performance based on such an evaluation alone.

This paper aims to quantify the uncertainties in the Cloud physical properties (CPP) retrieval algorithm of the climate monitoring satellite application facility (CMSAF), which uses the reflectances at 0.64 and 1.63 μm in the Nakajima and King (1990) method (see Fig. 2) to retrieve COT and r_{eff} , from which CWP can be calculated. The goal is to determine the circumstances under which the cloud properties retrievals from the CPP algorithm are sufficiently reliable for classical model evaluations over a large domain (e.g. Europe), i.e. stage I in Fig. 1. To achieve this goal, the retrieval uncertainties are quantified in a systematic way with respect to three effects that are known to affect the accuracy of Nakajima and King (1990) based retrievals: viewing geometry, multiple layer clouds and broken clouds. Note that three-dimensional cloud effects are not considered in this study; this paper focuses on providing information for the evaluation of climate models that are run over large domains at moderate resolutions ($\sim 25 \times 25 \text{ km}^2$), at which the uncertainties due to three-dimensional effects are supposed to be generally small (Zinner and Mayer, 2006).

To be able to perform this study a simulator for the MSG-SEVIRI instrument has been developed. This simulator is used to relate, over domains as large as Europe, the model-predicted three-dimensional cloudy atmosphere to the two-dimensional representation of this atmosphere in a satellite image. By using simulated satellite images for the retrieval of cloud properties, the differences between these retrievals and the model-predicted cloud parameters can be determined for a large variety of conditions of the cloudy atmosphere, and the sensitivities of these retrievals to e.g. multi-layer clouds can be examined in a systematic way (cf. stage III in Fig. 1).

The subject of this study has similarities with the study by Bugliaro et al. (2011) who used simulated radiances derived from a single model field generated with the regional consortium for small-scale modelling Europe (COSMO-EU) model. Their aim was to quantify errors in COT, r_{eff} and CWP retrievals from the algorithm for the physical investigation of clouds with SEVIRI (APICS) and the CPP algorithm. However, there are several differences in approach and methodology between their study and the one

Quantifying retrieval uncertainties in CPP

B. J. Jonkheid et al.

[Title Page](#)[Abstract](#)[Introduction](#)[Conclusions](#)[References](#)[Tables](#)[Figures](#)[◀](#)[▶](#)[◀](#)[▶](#)[Back](#)[Close](#)[Full Screen / Esc](#)[Printer-friendly Version](#)[Interactive Discussion](#)

Quantifying retrieval uncertainties in CPP

B. J. Jonkheid et al.

[Title Page](#)[Abstract](#)[Introduction](#)[Conclusions](#)[References](#)[Tables](#)[Figures](#)[◀](#)[▶](#)[◀](#)[▶](#)[Back](#)[Close](#)[Full Screen / Esc](#)[Printer-friendly Version](#)[Interactive Discussion](#)

presented here. First, in the current paper the retrieval errors are analysed in a more systematic way with respect to the effects of viewing geometry, multi-layer clouds and broken clouds, aiming to span the entire input space of the simulator. In contrast, Bugliaro et al. (2011) focus more on the comparison of two cloud properties retrieval algorithms on the basis of a single three-dimensional COSMO-EU cloud field to generate different cloud conditions. Second, the simulator presented here uses a different radiative transfer model (i.e. the doubling adding KNMI (DAK) model, Stammes, 2001) than the simulator used by Bugliaro et al. (2011) (i.e. the libRadtran model, Mayer and Kylling, 2005). The latter influenced the comparison results of Bugliaro et al. (2011), because part of the differences they found can be attributed to radiative transfer model differences between the CPP and APICS algorithms. Since in the current paper the radiative transfer models of the simulator and retrieval algorithm are identical these differences play no role. A more detailed comparison of the results of these studies will be discussed in the body of this paper.

This paper is organised as follows: in Sect. 2 the SEVIRI instrument is introduced, and the CPP retrieval algorithm which is used to analyse SEVIRI observations is described. Section 3 contains a brief description of the simulator used in this work. Section 4 discusses the results of the study, and in Sect. 5 the conclusions and outlook are given.

2 Data and methods

2.1 The SEVIRI instrument

The Spinning Enhanced Visible and Infrared Imager (SEVIRI) is a passive imager that is flown onboard Meteosat Second Generation (MSG), a series of geostationary satellites that are operated by the European Organization for the Exploitation of Meteorological Satellites (EUMETSAT). The SEVIRI instrument scans the complete disk of the Earth every 15 min, and operates three channels at visible and near infrared

wavelengths between 0.6 and 1.6 μm , eight channels at infrared wavelengths between 3.8 and 14 μm , and one high-resolution visible channel. The nadir spatial resolution of SEVIRI is $1 \times 1 \text{ km}^2$ for the high-resolution channel, and $3 \times 3 \text{ km}^2$ for the other channels.

5 2.2 Cloud physical properties retrieval algorithm

The cloud optical thickness (COT), the particle size (r_{eff}) and the cloud water path (CWP) are retrieved with the cloud physical properties algorithm (CPP) developed at the Royal Netherlands Meteorological Institute (KNMI) within the climate monitoring satellite application facility (CM-SAF) of EUMETSAT (Roebeling et al., 2006). The CPP algorithm retrieves these properties from visible, near-infrared and infrared radiances observed by passive imagers, such as the SEVIRI instrument onboard MSG, the Advanced Very High Resolution Radiometer (AVHRR) onboard the National Oceanic and Atmospheric Administration (NOAA) satellites, or the Moderate Resolution Imaging Spectroradiometer (MODIS) on board EOS Aqua or Terra.

The Nakajima and King (1990) method is used to retrieve COT and r_{eff} for cloudy pixels in an iterative manner by simultaneously comparing satellite observed reflectances at visible (0.6 μm) and near-infrared (1.6 μm) wavelengths to look-up tables (LUTs) of simulated reflectances of liquid water and ice clouds for given optical thicknesses, particle sizes and surface albedos (α_{surf}). The retrieval of cloud thermodynamic phase (ice or liquid water) is done simultaneously with the retrieval of COT and particle size. The ice phase is assigned to pixels for which the observed 0.6 and 1.6 μm reflectances correspond to simulated reflectances of ice clouds, and the cloud top temperature is lower than 265 K. The remaining cloudy pixels are considered to represent liquid water clouds (Wolters et al., 2008). Assuming vertically homogeneous clouds, the CWP is computed from the retrieved COT and r_{eff} . The retrievals are limited to satellite and solar viewing zenith angles smaller than 72° . At larger solar and viewing zenith angles the errors in the retrievals are too large due to the decreased accuracy of the radiative transfer simulations, the decreased signal to noise ratio of the reflectance observations, and

Quantifying retrieval uncertainties in CPP

B. J. Jonkheid et al.

Title Page

Abstract

Introduction

Conclusions

References

Tables

Figures

◀

▶

◀

▶

Back

Close

Full Screen / Esc

Printer-friendly Version

Interactive Discussion



the increased effect of three-dimensional cloud structures (Varnai and Marshak, 2007).

The LUTs have been generated with the Doubling Adding KNMI (DAK) radiative transfer model (Stammes, 2001). The optical thicknesses range from 0 to 256. Cloud droplets are assumed to be spherical with effective radii between 1 and 24 μm . For ice clouds, imperfect hexagonal ice crystals (Hess et al., 1998) are assumed with effective radii between 6 and 51 μm . Note that r_{eff} is defined slightly differently for ice crystals and liquid water droplets: for ice crystals, r_{eff} is the volume equivalent radius for a hexagonal column, while the radii of liquid water droplets are assumed to follow a gamma distribution with an effective variance of 0.15; the effective radius is defined as

$$r_{\text{eff}} = \left\langle r^3 \right\rangle / \left\langle r^2 \right\rangle, \text{ with } \langle \dots \rangle \text{ denoting an average over the size distribution.}$$

The MODTRAN model (Berk et al., 2000) is used to calculate, and correct for, the absorption by atmospheric trace gases on band-averaged reflectances as observed by satellite instruments (Meirink et al., 2009). The surface reflectance maps have been generated from five years of MODIS white-sky albedo data (Moody et al., 2008). The algorithm to separate cloud free from cloud contaminated and cloud filled pixels originates from the MODIS cloud detection algorithm (Ackerman et al., 1998; Platnick et al., 2003; Frey et al., 2008). It has been modified to make it applicable to other passive imagers and to make it independent from ancillary data.

Once COT and r_{eff} have been determined for a particular cloud, CWP can be calculated using $\text{CWP} = \frac{4}{3} \text{COT} r_{\text{eff}} / Q_{\text{ext}}$, where Q_{ext} is the extinction efficiency $Q_{\text{ext}} = \sigma_{\text{ext}} / \pi r_{\text{eff}}^2$ and σ_{ext} the extinction cross section of liquid water droplets or ice crystals of the appropriate size. It should be noted that Q_{ext} is almost uniformly two for droplets, so the expression simplifies to $\text{CWP} = \frac{2}{3} \text{COT} r_{\text{eff}}$, while for ice crystals it can range from two for small r_{eff} to 1.5 for larger crystals.

3 Simulator

Several simulators of satellite observations have already been developed, including the ISCCP simulator, the EarthCARE simulator, and the libRadtran software package.

Quantifying retrieval uncertainties in CPP

B. J. Jonkheid et al.

Title Page

Abstract

Introduction

Conclusions

References

Tables

Figures

◀

▶

◀

▶

Back

Close

Full Screen / Esc

Printer-friendly Version

Interactive Discussion



Quantifying retrieval uncertainties in CPP

B. J. Jonkheid et al.

[Title Page](#)[Abstract](#)[Introduction](#)[Conclusions](#)[References](#)[Tables](#)[Figures](#)[◀](#)[▶](#)[◀](#)[▶](#)[Back](#)[Close](#)[Full Screen / Esc](#)[Printer-friendly Version](#)[Interactive Discussion](#)

Each simulator is built for a different application, with some acting as a forward model while others simulate level 2 or level 3 satellite products. Although the aim is to generate the satellite reflectances as realistic as possible, assumptions have to be made which need to be taken into account when using the simulator. Therefore, a simulator can only be used to test algorithms that use the same assumptions. Moreover, the simulators differ with respect to resolution, ice crystal phase functions and overlap functions used.

The International Satellite Cloud Climatology Project (ISCCP) simulator was developed to convert cloud and atmosphere information from atmospheric models directly into the cloud information that is produced by the ISCCP project (e.g. Klein and Jakob, 1999; Webb et al., 2001; Tselioudis and Jakob, 2002). This project provides the first global climatology of cloud cover and cloud properties (COT, r_{eff} , CWP) at an acceptable spatial resolution of $30 \times 30 \text{ km}^2$ (Rossow and Garder, 1993; Rossow and Schiffer, 1999).

The EarthCARE simulator (ECSIM) is a computational tool which can simulate the complete EarthCARE mission (Voors et al., 2007; Donovan et al., 2008). ECSIM generates ground- and space-based radar and lidar observations as well as the satellite Bidirectional Reflectance Distribution Functions (BRDF) at the top of the atmosphere for the same cloud scenario. This simulator can simulate all the 4 instruments aboard the EarthCARE satellite, such as the 94 GHz cloud profiling radar, the high spectral resolution lidar at 353 nm, the multispectral imager and the broad-band radiometer. Cloud scenes, as input for the simulations, can be created using the embedded ECSIM cloud generator or they can be converted from Cloud Resolving Models or from Large Eddy Simulation models to ECSIM standard input cloud scene. ECSIM is developed for the simulations of small scale cloud fields, typically $10 \times 10 \text{ km}^2$.

The libRadtran software package was developed as a general atmospheric radiative transfer solver for wavelengths ranging from thermal infrared through the ultraviolet (Mayer and Kylling, 2005). The package includes a variety of solvers that can calculate radiances, irradiances or actinic fluxes in plane-parallel and pseudo-spherical 1-D

systems, or full three-dimensional Monte Carlo calculations. The various solvers can incorporate ice and liquid water clouds, aerosols, Rayleigh scattering and molecular absorption; the surface is usually treated Lambertian, although some solvers can also accommodate a specified surface BRDF.

5 The aforementioned simulators are not applicable in practice for the study under consideration here, for which accurate top of the atmosphere radiance calculations are required over a large domain (at least Europe) within a reasonable time frame. The simulator should eventually be capable of running concurrently with a weather or climate model in order to facilitate real-time comparisons, or run it on a long span of
10 climate model output to investigate its statistical properties. In general, explicit radiative transfer calculations take too long; instead, a simulator based on precalculated results in a lookup table, as applied in this study, is a much more efficient solution.

The SEVIRI simulator has been built to facilitate the evaluation of climate model predictions with SEVIRI data, with a focus on cloud physical properties such as CWP and particle size. Its main goal is to accurately and efficiently simulate reflectances at visible and near-infrared wavelengths (specifically at 0.64 and 1.63 μm , where the CPP algorithm performs its retrievals) for three-dimensional model cloud fields at regional to sub-global scales. To improve the computational performance of the simulator the radiative transfer is not carried out online; instead, the radiances are obtained by scanning a lookup table which has been set up in advance in a reduced parameter space.
20 To use this lookup table the vertical structure in each computational gridbox is reduced to a handful of parameters that contain the essential information. To work with model layers that are only partially cloudy, an independent column approximation using the stochastic cloud cover scheme by Räisänen et al. (2006) is used (see Fig. 3a): the grid box is divided into subcolumns; in any of the subcolumns, each layer is either completely cloudy or clear; the reflectance is calculated for each subcolumn independently, and the results are averaged to obtain the reflectance representative of the grid box. Further, each subcolumn has its vertical profiles of ice and liquid water content simplified to contain only the relevant information (see Fig. 3b): vertical profiles of water
25

Quantifying retrieval uncertainties in CPP

B. J. Jonkheid et al.

Title Page

Abstract

Introduction

Conclusions

References

Tables

Figures

I◀

▶I

◀

▶

Back

Close

Full Screen / Esc

Printer-friendly Version

Interactive Discussion



Quantifying retrieval uncertainties in CPP

B. J. Jonkheid et al.

Title Page

Abstract

Introduction

Conclusions

References

Tables

Figures

◀

▶

◀

▶

Back

Close

Full Screen / Esc

Printer-friendly Version

Interactive Discussion



droplets and ice crystals, each with its own profile of r_{eff} , are reduced to two layers: a liquid water layer at 2 km and/or an ice layer at 6 km. Each layer is given the optical thickness of the integrated vertical profile corresponding to its phase; r_{eff} is uniform in each layer, chosen in such a way that the layer has the same cloud water path as the vertical profile. If only a single thermodynamic phase is present in a given column, the calculations are performed for a single layer. The surface is always treated as a Lambertian reflector with the albedo given by the climate model.

The reflectances of the clouds constructed in this way are calculated with DAK. The geometries at which DAK reflectances are calculated are on a slightly different grid than is used for the CPP LUTs. This is done to avoid possibly biased results when using the retrieval algorithm on simulated reflectances. Note that although the LUTs of CPP and the simulator seem similar at a superficial level, the former does not allow both ice crystals and liquid water droplets to be present simultaneously whereas the latter does.

Once the cloud structure is simplified in this way, it can be parametrized with only four degrees of freedom: COT, optical ice fraction $f_{\text{ice}} = \text{COT}_{\text{ice}}/\text{COT}_{\text{total}}$, and r_{eff} of both liquid water droplets and ice crystals. Together with α_{surf} , solar and satellite zenith angles θ_0 and θ and sun-satellite azimuthal angle ϕ , this gives an 8-D lookup table from which the reflectances at 0.64 and 1.63 μm can be interpolated. The table has 44 grid points for both θ_0 and θ ; 91 grid points for ϕ ; 22 grid points for COT (0, and a range from 0.25 to 256); 10 grid points for the fractional ice content f_{ice} (0, and a range from 7.8×10^{-3} to 1); 3 grid points for surface albedo (0, 0.5 and 1); 2 grid points for $r_{\text{eff,liquid}}$ (10 and 13 μm); and 3 grid points for $r_{\text{eff,ice}}$ (30, 45 and 60 μm). Interpolation is done linearly, except for α_{surf} , for which the equation by Chandrasekhar (1960) was used:

$$R(\alpha_{\text{surf}}) = R(\alpha = 0) + \frac{\alpha_{\text{surf}} t(\theta_0) t(\theta)}{1 - \alpha_{\text{surf}} \alpha_{\text{hemi}}}$$

where R is the reflectance at the top of the atmosphere, $t(\theta_0)$ and $t(\theta)$ denote the

atmospheric transmissions at solar and satellite zenith angles, and α_{hemi} is the hemispherical sky albedo for upwelling isotropic radiation.

4 Results and discussion

4.1 Testing the CPP retrieval algorithm

5 To investigate the validity of the CPP retrieval algorithm, the simulator is used to obtain reflectances for a variety of input parameters. These reflectances are then used as input data of the CPP algorithm, and the retrieved cloud physical properties are compared to the original input. The emphasis is on the retrieval of CWP, using the retrievals of COT and r_{eff} only as intermediate steps. This choice was made because CWP is a more relevant quantity in climate models than COT and r_{eff} , and the underlying purpose is to gauge the usefulness of CPP in model evaluation.

15 In the following sections, both multiphase clouds and clouds containing only one layer of either ice or liquid water (labeled “pure ice” and “pure liquid water”) are studied, even though the latter two cases represent ideal situations where CPP should perform perfectly. The reason for this is twofold: first, the single-phase simulations provide a baseline error analysis with which other effects can be compared; for instance, retrievals of r_{eff} become uncertain for low values of COT, and this will be reflected in the analysis of single-phase clouds. Second, some sources of retrieval errors such as large solar zenith angles or broken clouds become more apparent if single-phase clouds are considered because these effects can then be considered the only sources of uncertainty.

4.1.1 Effects of solar zenith angle

20 As a first test the influence on the solar zenith angle on the CWP retrieval is examined for pure ice and pure liquid water clouds with a COT of either 6 or 100; α_{surf} was 0.1

Quantifying retrieval uncertainties in CPP

B. J. Jonkheid et al.

Title Page

Abstract

Introduction

Conclusions

References

Tables

Figures

◀

▶

◀

▶

Back

Close

Full Screen / Esc

Printer-friendly Version

Interactive Discussion



in all cases, while the effective radii of droplets and ice crystals are kept fixed at 11 and 38 μm , respectively. The resulting CWP retrieval errors, averaged over all satellite viewing angles with $\theta < 72^\circ$ on a grid consisting of 14 points in θ and 41 points in ϕ , are shown in Fig. 4. Three measures for the retrieval errors are used: the mean error, which indicates the bias of the retrievals; the RMS error, which indicates the accuracy of the retrievals; and the standard deviation, which indicates the precision of the retrievals. The quantities are given as dimensionless numbers, relative to the input CWP. In all cases the errors are averaged over all satellite geometries with $\theta < 72^\circ$, which is the largest zenith angle where CPP can still do meaningful retrievals.

It can be seen that liquid water clouds have generally low retrieval errors in these circumstances for most solar zenith angles. This is to be expected: the only differences between the simulated reflectances and those used in the CPP lookup tables are due to interpolation errors and the use of different grids in sun-satellite geometry and r_{eff} . There is an additional source of errors in the retrieval of the low COT clouds; due to uncertainties in the retrieval of r_{eff} at low optical thickness (cf. Fig. 2), CPP uses a weighted mean of the retrieved r_{eff} and a climatological mean of 8 μm for liquid water droplets and 26 μm for ice crystals. This effect becomes more pronounced for solar zenith angles greater than 50° . At higher COT values this effect disappears, since it is easier to retrieve r_{eff} there. The CWP retrieval errors for thin ice clouds mirror those of liquid water clouds, except there is less of an overall bias; at large solar zenith angles, there is a predominantly positive retrieval error in the forward scattering direction, while mainly negative for backscatter. For thick ice clouds, the CWP retrieval errors are larger than for liquid water clouds. This is caused by a overestimation of COT due to a combination of two effects: first, the ice clouds in the simulator are at 6 km, while CPP assumes all clouds to be at 2 km; this causes slight differences in the Rayleigh scattering occurring above the cloud, and hence different reflectances. The second effect can be seen in Fig. 2, where the reflectances at 0.6 μm for ice clouds saturate at a relatively low reflectance due to the small asymmetry factors of the Hess et al. (1998) ice crystals.

Quantifying retrieval uncertainties in CPP

B. J. Jonkheid et al.

[Title Page](#)[Abstract](#)[Introduction](#)[Conclusions](#)[References](#)[Tables](#)[Figures](#)[◀](#)[▶](#)[◀](#)[▶](#)[Back](#)[Close](#)[Full Screen / Esc](#)[Printer-friendly Version](#)[Interactive Discussion](#)

4.1.2 Effects of COT, multi-phase clouds and surface albedo

For a more thorough investigation of the effects of COT, α_{surf} and multiphase clouds (parametrised by the optical ice fraction f_{ice}), the reflectances are calculated for a parameter space spanning the relevant values of these parameters. This parameter space consists of a grid of 9 values of COT (ranging from 0.8 to 204.8), 7 values of f_{ice} (pure ice and pure liquid water clouds, plus five intermediate points ranging from $f_{\text{ice}} = 0.02$ to 0.8) and 5 values of α_{surf} (ranging from 0.05 to 0.8). Again, the effective radii of ice crystals and liquid water droplets are taken as 38 and 11 μm , respectively, and are assumed to be uniform within the cloud.

The CWP retrieval errors are illustrated in Figs. 5 and 6. As before, the retrieval errors are averaged over all satellite viewing angles with $\theta < 72^\circ$; now they are also averaged over all solar zenith angles with $\theta_0 < 72^\circ$ to focus more on the effects of the cloud and surface properties. It can be seen that retrieval errors are generally small for pure liquid water clouds, and to a lesser extend for pure ice clouds, generalising the results illustrated in Fig. 4. The only exceptions occur for low COT, caused by the aforementioned use in CPP of climatological mean values of r_{eff} , and for ice clouds with an optical thickness $\gtrsim 6$, caused by the fact that the simulator uses a different cloud top height from the CPP algorithm for ice clouds. As a result the COT retrievals for pure ice clouds are generally too high and quickly approach 256, the maximum COT value that CPP can retrieve. This explains the relatively high precision of the retrievals, and why the retrieval errors decrease as the input COT approaches this maximum value.

Retrievals of CWP are of a much lower quality in the case of multi-phase clouds, due to various reasons. The root of this problem is that CPP only defines a single phase for each retrieval, meaning it cannot interpret multi-phase clouds correctly. Even a thin ice cloud layer over a liquid water cloud layer can already introduce a large retrieval error: if the ice layer has enough optical thickness (typically with $\text{COT}_{\text{ice}} > 1$) the phase retrieval will interpret the entire COT of both layers as an ice cloud; even if the ice layer is optically thin, the different phase function of the ice crystals will introduce errors in the

Quantifying retrieval uncertainties in CPP

B. J. Jonkheid et al.

[Title Page](#)[Abstract](#)[Introduction](#)[Conclusions](#)[References](#)[Tables](#)[Figures](#)[◀](#)[▶](#)[◀](#)[▶](#)[Back](#)[Close](#)[Full Screen / Esc](#)[Printer-friendly Version](#)[Interactive Discussion](#)

retrieval when a pure liquid water cloud is assumed. This is illustrated in the second and third columns of Fig. 5, and in Fig. 6: for low values of f_{ice} (i.e. a thin ice cloud over a thick liquid water cloud), the CWP retrieval has the smallest error if the ice layer is still translucent and the phase retrieval is made for the bulk of the cloud. As the optical thickness of the ice layer increases, the ice crystals contribute more and more to the total cloud BRDF, interfering with the retrievals. When the ice layer becomes optically thick retrievals of COT show little errors because the cloud's BRDF matches with the retrieved cloud phase, and CWP errors are mainly caused by the mismatch between retrieved and bulk cloud values of r_{eff} . For larger values of f_{ice} the errors are lower, since the retrieved phase represents a greater part of the total cloudy column.

Varying the surface albedo has a limited effect on the CWP retrieval quality, increasing the uncertainties only at very high values ($\alpha_{surf} > 0.5$, i.e. snow-covered surfaces). For these bright surfaces the retrieval of COT becomes problematic because the contrast between the cloud and the surface decreases, leading to an overestimation of COT. This effect disappears when COT approaches a value of 256, the maximum value that CPP can retrieve.

4.1.3 Effects of fractional cloud cover

If a cloud is observed by the satellite, it will not necessarily fill the entire field of view. In general, a pixel that is interpreted as cloudy will have cloudy and clear parts, introducing uncertainties in the retrievals; specifically, r_{eff} is usually overestimated (Wolters et al., 2010; Zhang and Platnick, 2011) while COT and CWP are underestimated (Coakley et al., 2005). By construction this complication does not occur when simulating climate model fields, since the procedure outlined in Sect. 3 and Fig. 3 ensures that each subcolumn used in the calculations is either completely cloudy or completely clear; yet since it may occur in the observations, the uncertainties introduced when retrieving CWP for partially clouded pixels have to be assessed.

To study the effect of partial cloud cover in a pixel, the CWP retrieval error is determined for liquid water clouds with various values for COT, α_{surf} and cloud cover; pure

Quantifying retrieval uncertainties in CPP

B. J. Jonkheid et al.

Title Page

Abstract

Introduction

Conclusions

References

Tables

Figures

◀

▶

◀

▶

Back

Close

Full Screen / Esc

Printer-friendly Version

Interactive Discussion



Quantifying retrieval uncertainties in CPP

B. J. Jonkheid et al.

[Title Page](#)[Abstract](#)[Introduction](#)[Conclusions](#)[References](#)[Tables](#)[Figures](#)[◀](#)[▶](#)[◀](#)[▶](#)[Back](#)[Close](#)[Full Screen / Esc](#)[Printer-friendly Version](#)[Interactive Discussion](#)

liquid water clouds are chosen because they have the smallest intrinsic retrieval errors, hence the resulting errors can be considered to be mostly due to the fractional cloud cover. The resulting CWP retrieval errors are shown in Figs. 7 and 8. It can be seen that CWP retrieval errors rise dramatically for clouds with a relatively low COT or with very high COT, even at cloud fractions of 87.5%. Only clouds with COT ~ 10 over a dark surface have low retrieval errors; for these clouds, the overestimation of r_{eff} is found to compensate the underestimation of COT. Retrieval errors tend to increase even further with decreasing cloud fraction. Retrievals of CWP are generally too low due to underestimations of COT at low α_{surf} , and of r_{eff} at high α_{surf} . The only exception occurs at low COT and high α_{surf} , where the bright surface complicates COT retrievals with a high chance of overestimations.

4.2 Application to a climate model

A possible application of this work is to provide an uncertainty analysis on model cloud fields that one wants to compare with satellite data. To illustrate this, the simulator was used to obtain artificial SEVIRI observations and subsequent retrievals of a single climate model field using the Regional Atmospheric Climate Model (RACMO). RACMO is a hydrostatic limited-area model used for regional climate modeling; it has been developed at KNMI by porting the physics package of the ECMWF IFS (European Center for Medium-Range Weather Forecast Integrated Forecasting System), release cy23r4, into the forecast component of the HIRLAM (High Resolution Limited Area Model) NWP, version 5.0.6 (de Bruijn and van Meijgaard, 2005; van Meijgaard et al., 2008).

Figure 9 shows how the uncertainty analysis procedure is applied to a RACMO field across Western Europe, on 15 May 2009 at 12:00 UTC. For simplicity, the surface albedo used in this test at both 0.64 and 1.63 μm is adopted from the RACMO value for short-wave radiation. It is notable that most of the clouds in this scene, and nearly all clouds with an appreciable CWP, have both liquid water and ice phase represented. This can also be seen in the reflectancs, where the clouds which contain ice show up

as dark structures in the 1.63 μm channel while the liquid water clouds are brighter due to their smaller r_{eff} . However, this means that both the relative and absolute retrieval errors are generally large throughout the domain. This fact can be seen in the lower two panels of Fig. 9 where it is shown that nearly all clouds have their CWP overestimated by CPP. Notable exceptions occur in the pure liquid water clouds north west of the Iberian peninsula. As such, large differences between SEVIRI retrieved and model predicted CWP can be expected in those areas, even if the climate model were a perfect representation of reality. This result also emphasises that an evaluation of this model with satellite data should be conducted in the stages II or IV of Fig. 1, rather than stage I.

4.3 Comparison with other studies

The results of this study contrast with the findings of Bugliaro et al. (2011), who performed a similar study on the retrieval errors of COT, r_{eff} and CWP. In their paper, the libRadtran one-dimensional radiative transfer solver was used to simulate SEVIRI visible and near-infrared reflectances for a single downscaled three-dimensional cloud field produced by the COSMO-EU numerical weather prediction model. The retrieval errors were quantified by comparing the cloud properties retrieved by the CPP and the APICS algorithms, both applied to simulated SEVIRI reflectances, to the cloud properties in the COSMO-EU field.

One of the striking differences between their study and the present one is the much larger uncertainties Bugliaro et al. (2011) find for CPP retrievals of CWP. For liquid water clouds, they find a very broad distribution of differences between predicted and retrieved CWP values, with a width greater than the retrieved values and a tendency towards overestimation. This broad distribution of differences is most likely caused by uncertainties in the r_{eff} retrievals. This is mainly due to the abundance of optically thin clouds in their sample: for liquid water clouds, they have a mean COT of 9.13, so a sizeable portion of the clouds have COT values much smaller than 8. For these thin clouds, CPP will nudge its r_{eff} retrievals towards a climatological mean of 8 μm ; combined with

Quantifying retrieval uncertainties in CPP

B. J. Jonkheid et al.

Title Page

Abstract

Introduction

Conclusions

References

Tables

Figures

◀

▶

◀

▶

Back

Close

Full Screen / Esc

Printer-friendly Version

Interactive Discussion



Quantifying retrieval uncertainties in CPP

B. J. Jonkheid et al.

Title Page

Abstract

Introduction

Conclusions

References

Tables

Figures

I◀

▶I

◀

▶

Back

Close

Full Screen / Esc

Printer-friendly Version

Interactive Discussion



a mean r_{eff} in the model field of $5.32\ \mu\text{m}$ this will result in a positive bias in the CWP retrievals. This stands in stark contrast with the findings of the current paper, where generally higher COT values are considered and the retrievals for liquid water clouds show only very small uncertainties. For the thicker clouds, differences in the CWP uncertainties may also be caused by the assumptions made in each simulator and its interaction with CPP; for instance, the simulator presented here places liquid water clouds at 2 km height in a model atmosphere, as does CPP, whereas Bugliaro et al. (2011) allow for variable cloud top heights. Moreover, there may be differences between the droplet size distribution assumed by their simulator and the CPP algorithm, which might cause discrepancies as well.

Another difference between the two studies occurs with the CWP retrieval of ice clouds. This is again caused by low optical depth effects; for ice clouds the mean COT is 2.15, making this effect even more pronounced than for liquid water clouds. The mean r_{eff} is $41.32\ \mu\text{m}$, meaning that the assumption in CPP of a climatological mean value of $26\ \mu\text{m}$ for optically thin ice clouds can explain the underestimation of CWP. Also, their simulator uses different phase functions for ice crystals than CPP, while in the current paper the same type of crystals are used (albeit with different values of r_{eff}). For multi-phase clouds the two studies agree that CWP retrieval uncertainties are relatively large.

It is noteworthy that the APICS retrievals shown in Bugliaro et al. (2011) are generally more accurate and precise than the CPP retrievals. While the present paper offers no such comparison, it should be noted that the two studies are not necessarily neutral with respect to the retrieval algorithm used. Both APICS and the simulator applied in Bugliaro et al. (2011) are based on the libRadtran radiative transfer model, while both CPP and the simulator developed here are based on the DAK code. This set-up likely causes subtle biases in the interactions between the simulator and the retrieval algorithm, for example in the ice crystal scattering phase functions and the droplet size distribution.

5 Conclusions

Retrievals of cloud water path (CWP) with the CPP algorithm work well for pixels that are completely covered by either pure ice or pure liquid water clouds with cloud optical thickness $COT > 5$. For ice clouds, the retrieval error is within 10% when $COT < 80$; liquid water clouds have comparable retrieval errors up to $COT = 200$. A very high surface albedo (> 0.5) leads to larger uncertainties. The CWP retrieval errors show little variation for $\theta < 50^\circ$, and tend to increase for larger values of θ .

For multi-phase clouds, CWP retrievals become very sensitive to errors when there is a thin ice cloud overlying a thick liquid water cloud. With such multi-phase clouds, an acceptable retrieval of CWP can only be carried out for very low values of the optical ice fraction f_{ice} , where the ice layer is optically thin and does not interfere with the observation of the liquid water layer, and for high values of f_{ice} (> 0.6), where the ice layer represents the majority of the observed cloud. These uncertainties arise from the fact that the CPP cloud phase retrievals focus on a few optical depths at the top of the cloud; in carrying out a CWP retrieval it applies this information to the whole cloud using the method outlined in Sect. 2.2.

When a cloud covers only part of the SEVIRI pixel, the CWP retrievals show a considerable negative bias for cloud fractions $< 80\%$. The precision in the retrievals is quite good, however, indicating that the effects of broken cloud cover can be compensated if the cloud fraction is known somehow.

While some of the results presented here are in contrast with the findings of Bugliaro et al. (2011), who performed a similar study, these discrepancies can be explained by differences in the experimental set-ups and assumptions that go into the respective simulators.

Acknowledgements. This work is part of the project titled “Construction and application of an MSG/SEVIRI simulator” that is carried out in the User Support Programme Space Research under the supervision of the Netherlands Space Office (NSO). We wish to thank Piet Stammes for the use of the DAK radiative transfer code. We would also like to thank Brent Maddux, Piet Stammes, Wouter Greuell and Jan Fokke Meirink for reviewing earlier versions of this

Quantifying retrieval uncertainties in CPP

B. J. Jonkheid et al.

Title Page

Abstract

Introduction

Conclusions

References

Tables

Figures

◀

▶

◀

▶

Back

Close

Full Screen / Esc

Printer-friendly Version

Interactive Discussion



manuscript. Further, we thank Jérôme Riédi for providing the SEVIRI cloud detection code, and Olaf Tuinder for his help with technical issues.

References

- Ackerman, S., Strabala, K., Menzel, W., Frey, R., Moeller, C., and Gumley, L.: Discriminating clear sky from clouds with MODIS, *J. Geophys. Res.*, 103, 32141–32157, 1998. 4317
- Berk, A., Anderson, G., Acharya, P., Chetwynd, J., Bernstein, L., Shettle, E., Matthew, M., and Adler-Golden, S.: MODTRAN4 Version 2 Users Manual, Tech. rep., Air Force Research Laboratory, 2000. 4317
- Bugliaro, L., Zinner, T., Keil, C., Mayer, B., Hollmann, R., Reuter, M., and Thomas, W.: Validation of cloud property retrievals with simulated satellite radiances: a case study for SEVIRI, *Atmos. Chem. Phys.*, 11, 5603–5624, doi:10.5194/acp-11-5603-2011, 2011. 4314, 4315, 4326, 4327, 4328
- Chandrasekhar, S.: Radiative Transfer, Dover Publications, Dover, 1960. 4320
- Coakley, J., Friedman, M., and Tahnk, W.: Retrieval of cloud properties for partly cloudy imager pixels, *J. Atmos. Ocean. Tech.*, 22, 3–17, 2005. 4324
- de Bruijn, E. and van Meijgaard, E.: Verification of HIRLAM with ECMWF physics compared with HIRLAM reference versions, HIRLAM Tech. Rep. 63, available from SMHI, S-601 76 Norrköping, Sweden, 2005. 4325
- Donovan, D., Voors, R., van Zadelhoff, G.-J., and Acarreta, J.: ECSIM Models and Algorithms Document, Tech. Rep., 2008. 4318
- Frey, R., Ackerman, S., Liu, Y., Strabala, K., Zhang, H., Key, J., and Wang, X.: Cloud detection with MODIS. Part I: Improvements in the MODIS Cloud Mask for Collection 5, *J. Atmos. Ocean. Tech.*, 25, 1057–1072, 2008. 4317
- Greuell, W., van Meijgaard, E., Meirink, J., and Clerbaux, N.: Evaluation of model predicted top-of-atmosphere radiation and cloud parameters over Africa with observations from GERB and SEVIRI, *J. Climate*, 24, 4015–4036, 2011. 4313
- Hess, H., Koелеmeijer, R., and Stammes, P.: Scattering matrices of imperfect hexagonal crystals, *J. Quant. Spectrosc. Ra.*, 60, 301–308, 1998. 4317, 4322
- Klein, S. and Jakob, C.: Validation and sensitivities of frontal clouds simulated by the ECMWF model, *Month. Weather Rev.*, 127, 2514–2531, 1999. 4318

Quantifying retrieval uncertainties in CPP

B. J. Jonkheid et al.

Title Page

Abstract

Introduction

Conclusions

References

Tables

Figures

◀

▶

◀

▶

Back

Close

Full Screen / Esc

Printer-friendly Version

Interactive Discussion



- Mayer, B. and Kylling, A.: Technical note: The libRadtran software package for radiative transfer calculations – description and examples of use, *Atmos. Chem. Phys.*, 5, 1855–1877, doi:10.5194/acp-5-1855-2005, 2005. 4315, 4318
- Meirink, J., Roebeling, R., and van Meijgaard, E.: Atmospheric correction for the KNMI cloud physical properties retrieval algorithm, *Tech. Rep. TR-304*, KNMI, 2009. 4317
- Molders, N., Laube, M., and Raschke, E.: Evaluation of model generated cloud cover by means of satellite data, *Atmos. Res.*, 39, 91–111, 1995. 4313
- Moody, E., King, M., Schaaf, C., and Platnick, S.: MODIS-Derived Spatially Complete Surface Albedo Products: Spatial and Temporal Pixel Distribution and Zonal Averages, *J. Appl. Meteorol. Clim.*, 47, 2879–2894, 2008. 4317
- Nakajima, T. and King, M.: Determination of the Optical Thickness and Effective Particle Radius of Clouds from Reflected Solar Radiation Measurements. Part 1: Theory, *J. Atmos. Sci.*, 47, 1878–1893, 1990. 4314, 4316, 4333
- Platnick, S., King, M., Ackerman, S., Menzel, W., Baum, B., Riedi, J., and Frey, R.: The MODIS cloud products: algorithms and examples from Terra, *IEEE Trans. Geosci. Remote Sens.*, 41, 459–473, 2003. 4317
- Räsänen, P., Barker, H., Khairoutdinov, M., Li, J., and Randall, D.: Stochastic generation of subgrid-scale cloudy columns for large-scale models, *Q. J. Roy. Meteor. Soc.*, 130, 2047–2067, 2006. 4319, 4334
- Roebeling, R. and van Meijgaard, E.: Evaluation of the daylight cycle of model predicted cloud amount and condensed water path over Europe with observations from MSG-SEVIRI, *J. Climate*, 22, 1749–1766, 2009. 4313
- Roebeling, R., Feijt, A., and Stammes, P.: Cloud property retrievals for climate monitoring: implications of differences between Spinning Enhanced Visible and Infrared Imager (SEVIRI) on METEOSAT-8 and Advanced Very High Resolution Radiometer (AVHRR) on NOAA-17, *J. Geophys. Res.*, 111, D20210, doi:10.1029/2005JD006990, 2006. 4312, 4316
- Rossow, W. and Garder, L.: Cloud detection using satellite measurements of infrared and visible radiances from ISCCP, *J. Climate*, 6, 2341–2369, 1993. 4318
- Rossow, W. and Schiffer, R.: Advances in understanding clouds from ISCCP, *B. Am. Meteorol. Soc.*, 80, 2261–2287, 1999. 4318
- Stammes, P.: Spectral radiance modeling in the UV-Visible range, in: *IRS 2000: current problems in atmospheric radiation*, edited by: Smith, W. and Timofeyev, Y., A. Deepak Publ., Hampton, Va, 385–388, 2001. 4315, 4317

Quantifying retrieval uncertainties in CPP

B. J. Jonkheid et al.

Title Page

Abstract

Introduction

Conclusions

References

Tables

Figures

◀

▶

◀

▶

Back

Close

Full Screen / Esc

Printer-friendly Version

Interactive Discussion



Quantifying retrieval uncertainties in CPP

B. J. Jonkheid et al.

[Title Page](#)[Abstract](#)[Introduction](#)[Conclusions](#)[References](#)[Tables](#)[Figures](#)[◀](#)[▶](#)[◀](#)[▶](#)[Back](#)[Close](#)[Full Screen / Esc](#)[Printer-friendly Version](#)[Interactive Discussion](#)

- Tselioudis, G. and Jakob, C.: Evaluation of midlatitude cloud properties in a weather and a climate model: Dependence on dynamic regime and spatial resolution, *J. Geophys. Res.*, 107, 4781, doi:10.1029/2002JD002259, 2002. 4313, 4318
- van Meijgaard, E., van Ulft, L., van de Berg, W., Bosveld, F. C., van den Hurk, B., Lenderink, G., and Siebesma, A.: The KNMI regional atmospheric climate model RACMO version 2.1, Tech. Rep. TR-302, KNMI, 2008. 4325
- Varnai, T. and Marshak, A.: View angle dependence of cloud optical thickness retrieved by MODIS, *J. Geophys. Res.*, 112, D06203, doi:10.1029/2005JD006912, 2007. 4317
- Voors, R., Donovan, D., Acarreta, J., Eisinger, M., Franco, R., Lajas, D., Moyano, R., Pirondini, F., Ramos, J., and Wehr, T.: ECSIM: the simulator framework for EarthCARE, in: *Proc. SPIE* 6744, 2007. 4318
- Webb, M., Senior, C., Bony, S., and Morcrette, J.-J.: Combining ERBE and ISCCP data to assess clouds in the Hadley Centre, ECMWF and LMD climate models, *Clim. Dynam.*, 17, 905–922, 2001. 4318
- Wolters, E., Roebeling, R., and Feijt, A.: Evaluation of cloud-phase retrieval methods for SEVIRI using ground-based lidar and cloud radar data, *J. Appl. Meteorol. Clim.*, 47, 1723–1738, 2008. 4316
- Wolters, E., Deneke, H., van der Hurk, B., Meirink, J., and Roebeling, R.: Broken and inhomogeneous cloud impact on satellite cloud particle effective radius and cloud-phase retrievals, *J. Geophys. Res.*, 115, D10214, doi:10.1029/2009JD012205, 2010. 4324
- Zhang, Z. and Platnick, S.: An assessment of differences between cloud effective particle radius retrievals for marine water clouds from three MODIS spectral bands, *J. Geophys. Res.*, 116, D20215, doi:10.1029/2011JD016216, 2011. 4324
- Zinner, T. and Mayer, B.: Remote sensing of stratocumulus clouds: Uncertainties and biases due to inhomogeneity, *J. Geophys. Res.*, 111, D14209, doi:10.1029/2005JD006955, 2006. 4314

Quantifying retrieval uncertainties in CPP

B. J. Jonkheid et al.

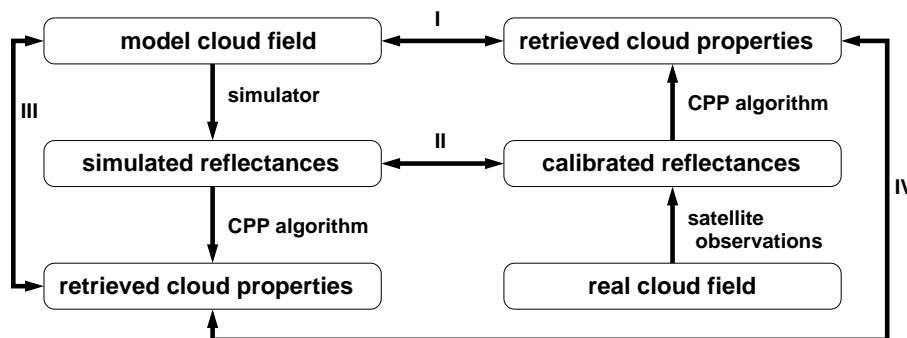


Fig. 1. Diagram of the comparison of model cloud fields with observations. The left side represents the model, with simulated observations and retrievals on the simulated field; the right side represents the observations, with the retrieved properties of real clouds. The double-headed arrows represent stages at which comparisons can be performed. It should be noted that stage III does not involve any reference to the real cloud field, but it can be used to diagnose the model-simulator-retrieval chain.

Title Page

Abstract

Introduction

Conclusions

References

Tables

Figures

◀

▶

◀

▶

Back

Close

Full Screen / Esc

Printer-friendly Version

Interactive Discussion



Quantifying retrieval uncertainties in CPP

B. J. Jonkheid et al.

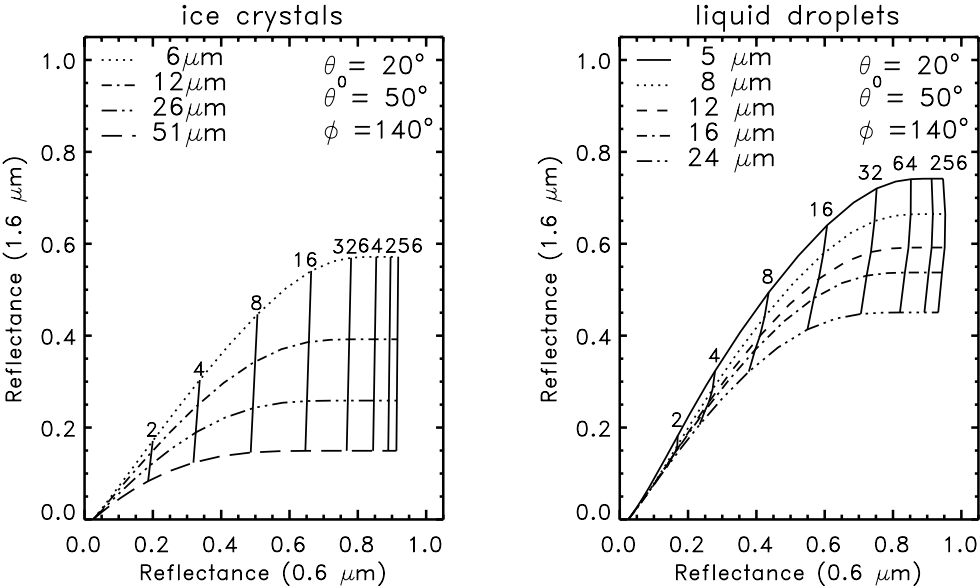


Fig. 2. The Nakajima and King (1990) retrieval method. Each curve shows the values of reflectances at 0.64 and 1.63 μm for a certain value of r_{eff} as a function of COT (indicated by the mostly vertical lines). Thus, from a combination of these reflectances both the COT and r_{eff} of a cloud can be determined. The left panel shows the retrieval curves for ice crystals, the right panel for water droplets; the viewing geometry is indicated in the upper right of each panel.

Discussion Paper | Discussion Paper | Discussion Paper | Discussion Paper | Discussion Paper

Title Page

Abstract Introduction

Conclusions References

Tables Figures

◀ ▶

◀ ▶

Back Close

Full Screen / Esc

Printer-friendly Version

Interactive Discussion



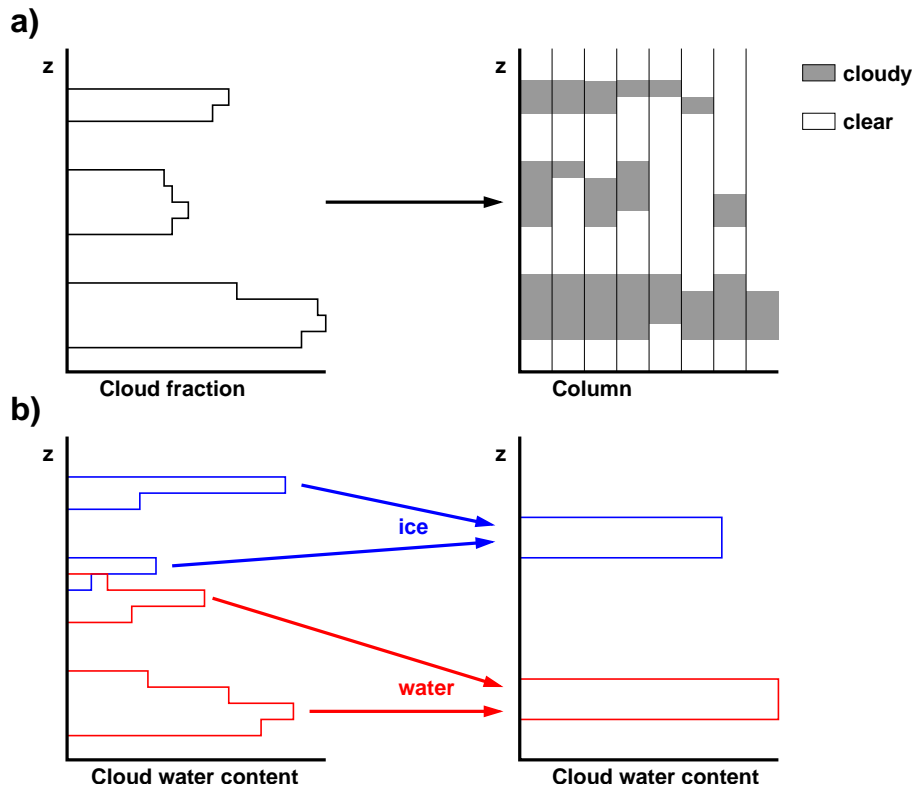


Fig. 3. Simplifications made to the cloud structure in the SEVIRI simulator: **(a)** each model grid cell is divided into subcolumns; in each subcolumn, a model layer that has a non-zero cloud fraction is either completely cloudy or completely clear following the stochastic method of Räsänen et al. (2006); **(b)** in each subcolumn all the ice is put into a single layer at 6 km, while all the liquid water is put into a single layer at 2 km.

Quantifying retrieval uncertainties in CPP

B. J. Jonkheid et al.

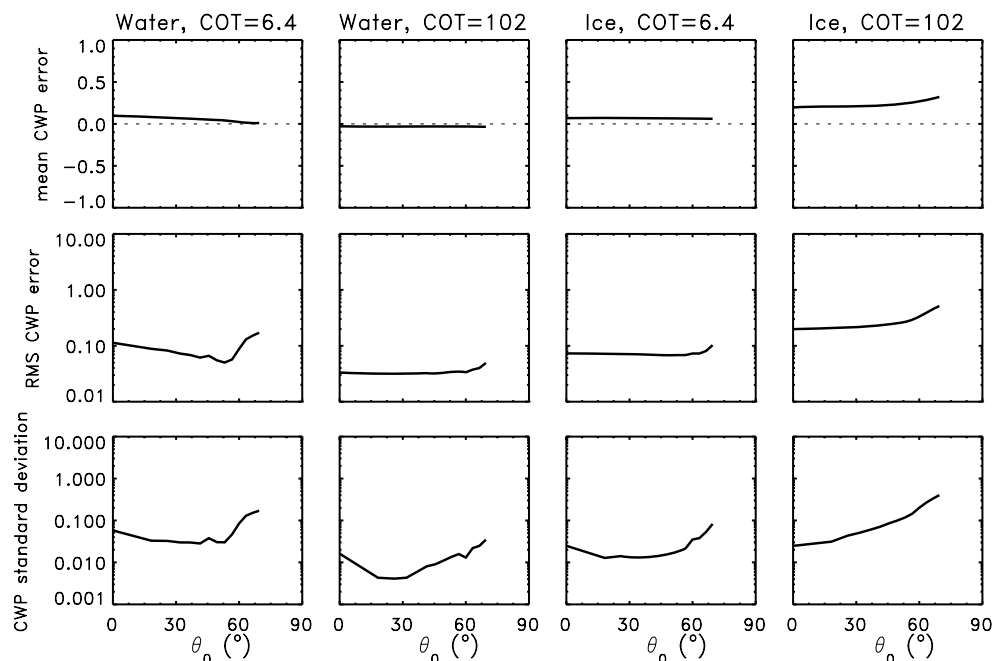


Fig. 4. The CWP retrieval errors as a function of solar zenith angle θ_0 , for different pure liquid water and pure ice clouds (indicated at the top of each column). The top row shows the mean relative error (indicative of the bias of the retrievals); the middle row shows the RMS relative error (indicative of the accuracy of the retrievals); the lower row shows the standard deviation (indicative of the precision of the retrievals). Results were averaged over all satellite geometries with $\theta < 72^\circ$; the effective radii are $r_{\text{eff}} = 11 \mu\text{m}$ for liquid water clouds and $r_{\text{eff}} = 38 \mu\text{m}$ for ice clouds.

Title Page

Abstract

Introduction

Conclusions

References

Tables

Figures

◀

▶

◀

▶

Back

Close

Full Screen / Esc

Printer-friendly Version

Interactive Discussion



Quantifying retrieval uncertainties in CPP

B. J. Jonkheid et al.

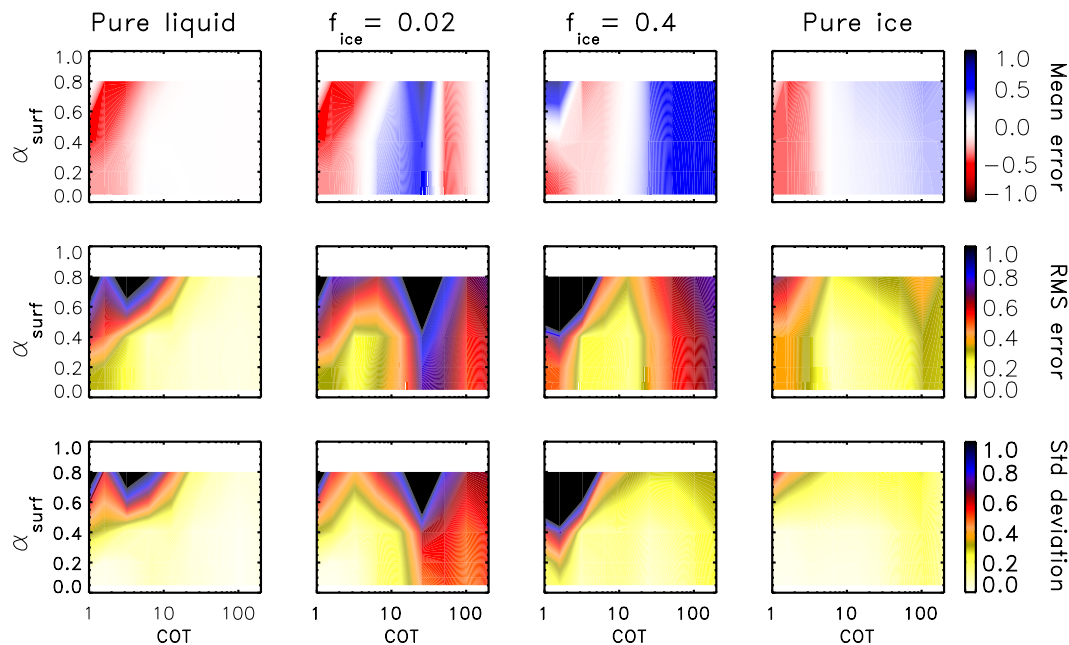


Fig. 5. The CWP retrieval errors as a function of COT and α_{surf} , averaged over all satellite viewing angles with $\theta < 72^\circ$ and solar zenith angles with $\theta_0 < 72^\circ$. The columns indicate different values of f_{ice} , while the rows are as in Fig. 4. Again, effective radii are $r_{\text{eff}} = 11 \mu\text{m}$ for liquid water clouds and $r_{\text{eff}} = 38 \mu\text{m}$ for ice clouds.

Title Page

Abstract

Introduction

Conclusions

References

Tables

Figures

◀

▶

◀

▶

Back

Close

Full Screen / Esc

Printer-friendly Version

Interactive Discussion



Quantifying retrieval uncertainties in CPP

B. J. Jonkheid et al.

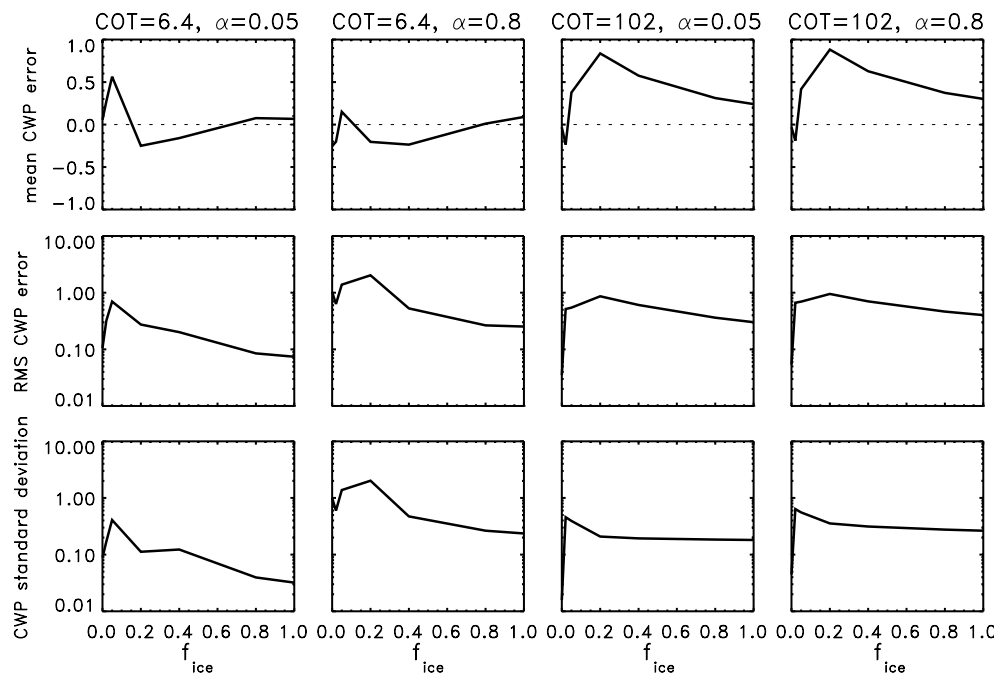


Fig. 6. As Fig. 5, except the errors are shown as functions of f_{ice} for several combinations of COT and α_{surf} .

Title Page

Abstract

Introduction

Conclusions

References

Tables

Figures

◀

▶

◀

▶

Back

Close

Full Screen / Esc

Printer-friendly Version

Interactive Discussion



Quantifying retrieval uncertainties in CPP

B. J. Jonkheid et al.

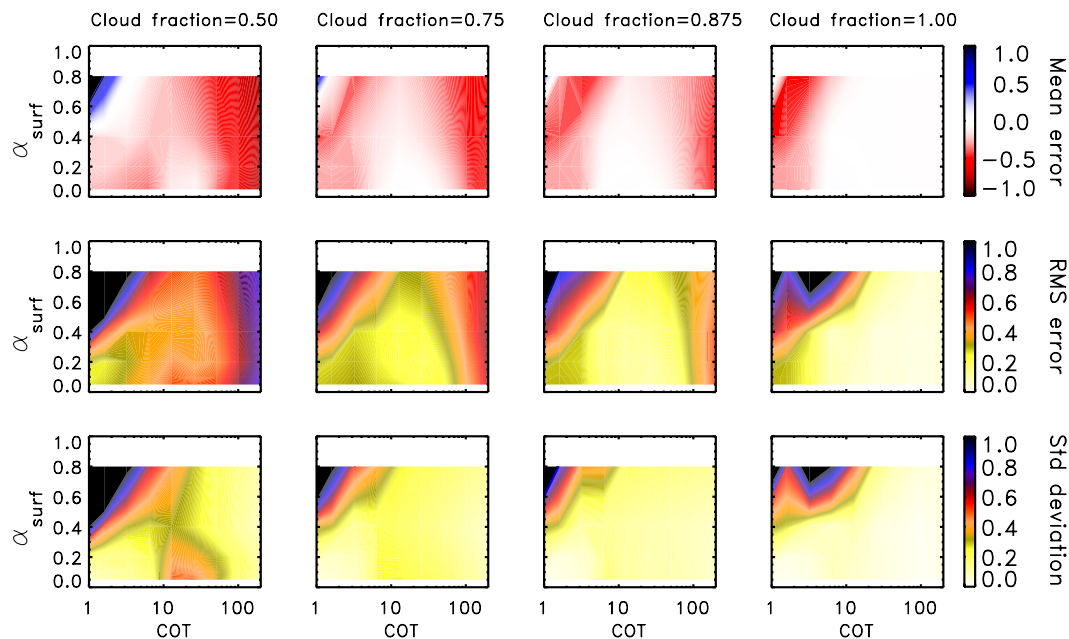


Fig. 7. As Fig. 5, except the results are for pure liquid water clouds, and the columns indicate different values of the cloud fraction.

Title Page

Abstract

Introduction

Conclusions

References

Tables

Figures

◀

▶

◀

▶

Back

Close

Full Screen / Esc

Printer-friendly Version

Interactive Discussion



Quantifying retrieval uncertainties in CPP

B. J. Jonkheid et al.

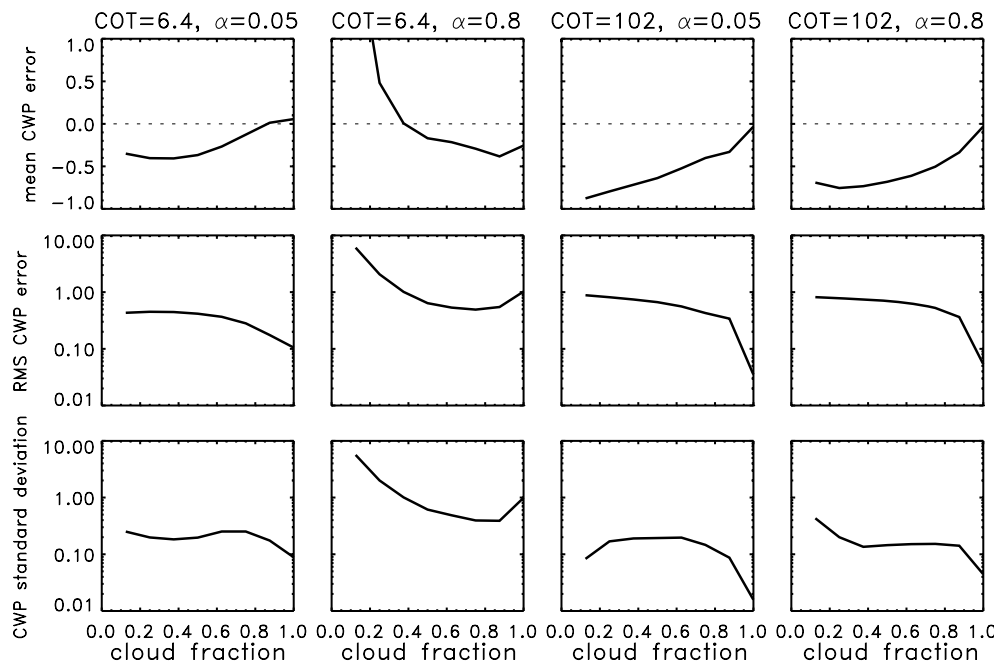


Fig. 8. As Fig. 7, except the errors are shown as functions of the cloud fraction for several combinations of COT and α_{surf} .

Title Page

Abstract

Introduction

Conclusions

References

Tables

Figures

◀

▶

◀

▶

Back

Close

Full Screen / Esc

Printer-friendly Version

Interactive Discussion



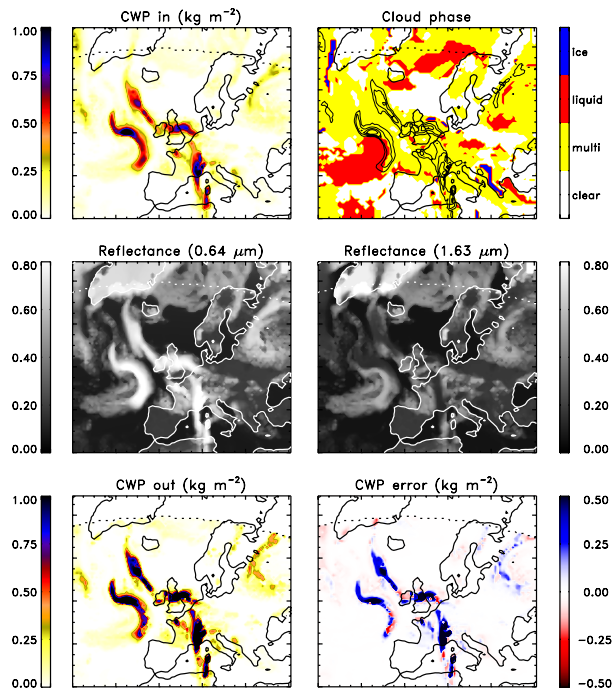


Fig. 9. Application of the simulator to a single RACMO field, for 15 May 2009, 12:00 UTC. The upper left panel gives the CWP calculated by RACMO; the upper right panel gives the cloud phase at each grid point (>99 % ice, >99 % liquid water, multi-phase, or clear), with contours tracing CWP for ease of reference; the center left panel gives the simulated reflectance at $0.64 \mu\text{m}$; the center right panel gives the simulated reflectance at $1.63 \mu\text{m}$; the lower left panel gives the retrieved CWP after the RACMO output was put through the simulator and CPP; the lower right panel gives the difference between the retrieved CWP and the RACMO CWP. In all panels the dotted line marks the area where both the solar and satellite zenith angles are less than 72° ; no retrievals are done beyond this line.

Quantifying retrieval uncertainties in CPP

B. J. Jonkheid et al.

Title Page

Abstract Introduction

Conclusions References

Tables Figures

◀ ▶

◀ ▶

Back Close

Full Screen / Esc

Printer-friendly Version

Interactive Discussion

